Contribution from the University of Manchester
Institute of Science and Technology, Manchester M60 1QD, U.K.

Effect of Crystal Structure and Percentage of Ion Exchange on ESR Spectra of Hydrated Fe(III) Ion Exchanged Synthetic Zeolites

N. P. Evmiridis[†]

Received February 25, 1986

Fe(III) ion exchanged A and X type crystalline zeolites in hydrated form have been investigated by using ESR techniques. Two main signals were observed, a broad signal centered around $g = 2.0$ and a sharp signal at $g \simeq 4.3$. The broad signal was attributed to the $M_s = -1/2 \leftrightarrow M_s = +1/2$ transition of the Hamiltonian $\mathcal{H} = g\beta HS + D[S_z^2 - 1/3S(S+1)] + E[S_x^2 - S_y^2]$, and it is likely to be contributed from distributions of crystal field parameters. The distribution mean value of E/D is considered greater than $1/9$ on the basis of its shape while that of $D/h\nu$ is calculated to be in the range 0.23-0.26. The Fe(III) ions contributing to this broad signal were assigned to ions associated with the zeolite framework. The signal at $g \simeq 4.3$ was attributed to the $M_s = +1/2 \leftrightarrow M_s = -1/2$ transition of the same Hamiltonian with $D/h\nu > 0.35$ and $E/D = 1/3$. The dependence of relative intensities on the extent of exchange indicated that the Fe(III) ions associated with the zeolite framework reserved the low coordination symmetry regardless of the extent of exchange or type of zeolitic structure. The Fe(III) species contributing to $g \simeq 4.3$ were associated with Fe(III) ions replacing Al(III) in the zeolitic framework. These Fe(III) ions were incorporated into the zeolitic structure during synthesis and consequently were present in the zeolitic structure prior to Fe(III) ion exchange. Contributions from framework Fe(III) ions to the $g \simeq 4.3$ signal were found in both A and X type. In the case of X type zeolite an additional contribution to the signal with $g \simeq 4.3$ arose from Fe(III) ions involved in an amorphous phase, which developed during the ion-exchange process and was dependent on the percentage of exchange.

Introduction

Zeolites are inorganic polymer anions made of tetrahedra of SiO_4 and AlO_4 cross-linked together in various ways to form crystalline structures with Si, Al, and O as the main framework elements. The negative charge of the anion is balanced from the charge of small cations, which enter the structure and are localized in interstitial sites, the positions of which are determined from potential energy wells of the anion structure in the nearby space. Figure 1 shows the zeolitic structure together with metal ion localization sites for A, X, and Y type zeolites.

ESR spectroscopy is useful for identifying the metal ion localization site in zeolites when the introduced ion is paramagnetic. This leads to the experimental finding of the energetically favorable positions of the interstitial space to accommodate positive ions. In addition, from X-ray diffraction data, it has been found that the different metal ions are localized in different proportions among the available sites of a particular zeolitic structure.[1-9] This selectivity in localization site of individual metal ions is important in heterogeneous catalysis. Fe(III) ions in various solid matrices catalyze oxidations and Fe(III) ion exchanged zeolites have been found to be active for deep and selective oxidation processes[10-12] also. γ-Resonance spectroscopy was found to be an easy method to detect the oxidation state and the coordination symmetry of the iron species, especially when only one coordination symmetry is involved in each oxidation state. Zeolites with Fe(III) metal ions exchanged for Na(I) or NH_4^+ have been synthesized[13-17] and intensively studied by γ-resonance spectroscopy.[17-22] Delgass and co-workers[19] showed that vacuum dehydration of Fe-Na-Y zeolites reduces Fe(III) to Fe(II), which then move to sites I and II of the zeolitic structure. Mössbauer studies made recently by Rees and co-workers[21,22] showed that Fe(III) ions in hydrated Fe(III) ion exchanged zeolites produced from oxidation of Fe(II) ions were found in octahedral coordination symmetry. However, the Mössbauer technique lacks sensitivity and needs laborious computation programs when iron species of both oxidation states and several coordination symmetries are involved. On the other hand ESR is a very sensitive technique and can be used whenever such sensitivity is of importance. One of the first research groups to use ESR spectra for metal ion localization site identification was the group of Kazanskii and co-workers.[23] From ESR and corresponding optical spectra they were able to follow the change of localization position of different ions with dehydration. Specifically, for the 3+ ions they argued that ions, on partial dehydration, tend to localize in sites near the walls of the supercage with square-pyramidal or distorted-octahedral coordination and on further dehydration they penetrate to sites in the small pore region, with distorted-tetrahedral coordination.

The Fe(III) high-spin ion with $^6S_{5/2}$ ($3d^5$) ground state can give rise to ESR signals that, in low-symmetry ligand fields, show fine structure. Additionally it has been shown that the zeolitic structure may suffer breakdown during Fe(III) ion exchange, the extent of which depends on the type of zeolitic structure, the percentage of exchange, and the conditions of the ion-exchange process.[24] This breakdown phenomenon produces in some cases a cluster

[†] Present address: Chemistry Department, University of Ioannina, Ioannina, Greece.

(1) Eluenberger, G. R.; Shoemaker, D. R.; Keil, J. G. *J. Phys. Chem.* **1967**, *71*, 1872.
(2) Smith, J. V.; Bennett, J. M.; Flanegan, E. M. *Nature (London)* **1967**, *215*, 241.
(3) Olson, D. H.; Kokotail, L.; Charnell, J. F. *J. Colloid Interface Sci.* **1968**, *28*, 305.
(4) Olson, D. H.; Sherry, H. S. *J. Phys. Chem.* **1968**, *72*, 4095.
(5) Olson, D. H. *J. Phys. Chem.* **1968**, *72*, 4366.
(6) Mortier, J.; Bosman, H. J. *J. Phys. Chem.* **1971**, *75*, 3327.
(7) Mortier, J.; Bosman, H. J.; Uytherhoeven, J. B. *J. Phys. Chem.* **1972**, *76*, 650.
(8) Gallezot, P.; Imelik, B. *J. Chim. Phys. Phys.-Chim. Biol.* **1971**, *68*, 34.
(9) Evmerides, N. P.; Beagley, B.; Dwyer, J. *Inorg. Chim. Acta* **1976**, *20*, 243.
(10) Scalcina, I. V.; Kolchim, I. K.; Margolis, Ya. L.; Ermolenko, N. F.; Levina, S. A.; Halashwick, L. N. *Izv. Akad. Nauk SSSR, Ser. Khim.* **1970**, *5*, 929.
(11) Scalcina, I. V.; Kolchim, I. K.; Margolis, Ya. L.; Ermolenko, N. F.; Levina, S. A.; Halashwick, L. N. *Kinet. Katal.* **1958**, *10*, 185.
(12) Scalcina, I. V.; Kolchim, I. K.; Margolis, Ya. L.; Ermolenko, N. F.; Levina, S. A.; Halashwick, L. N. *U.S.S.R. Patent* **1968**, *239*, 929; *Chem. Abstr.* **1969**, *70* 28407.
(13) Wichterlová, B.; Novaková, J.; Kubelcová, L.; Mikušik, P. *Zeolites* **1985**, *5*, 21.
(14) Novaková, J.; Kubelcová, L.; Wichterlová, B.; Juška, T.; Dolejsek, Z. *Zeolites* **1982**, *2*, 17.
(15) Badran, A. H.; Dwyer, J.; Evmerides, N. P.; Manford, J. A. *Inorg. Chim. Acta* **1977**, *21*, 61.
(16) Wichterlová, B.; Kubelcová, L.; Jiřu, P.; Kolichová, D. *Collect. Czech. Chem. Commun.* **1980**, *45*, 2143.
(17) Morrice, J. A.; Rees, L. V. C. *Trans. Faraday Soc.* **1968**, *64*, 1388.
(18) Gol'danski, V. I.; Suzdalev, I. P.; Plachindas, A. S.; Shtyrkov, B. G. *Dokl. Adak. Nauk. SSSR* **1966**, *169*, 872.
(19) Delgass, W. V.; Garten, R. L.; Boudart, M. *J. Phys. Chem.* **1969**, *73*, 2976.
(20) Brandt, R.; Mehner, H.; Ebert, I. *Z. Anorg. Allg. Chem.* **1982**, *486*, 229.
(21) Dickson, B.; Rees, L. V. C. *J. Chem. Soc., Faraday Trans. 1* **1974**, *70*, 2038.
(22) Gao, Z.; Rees, L. V. C. *Zeolites* **1982**, *2*, 215.
(23) Kazanskii, V.; Mikheikin, I. *Izv. Otd. Khim. Nauki (Bulg. Akad. Nauk.)* **1 73**, *6*, 361.
(24) Badran, A. H.; Dwyer, J.; Evmerides, N. P. *Inorg. Chim. Acta* **1977**, *21*, 233.

0020-1669/86/1325-4362$01.50/0

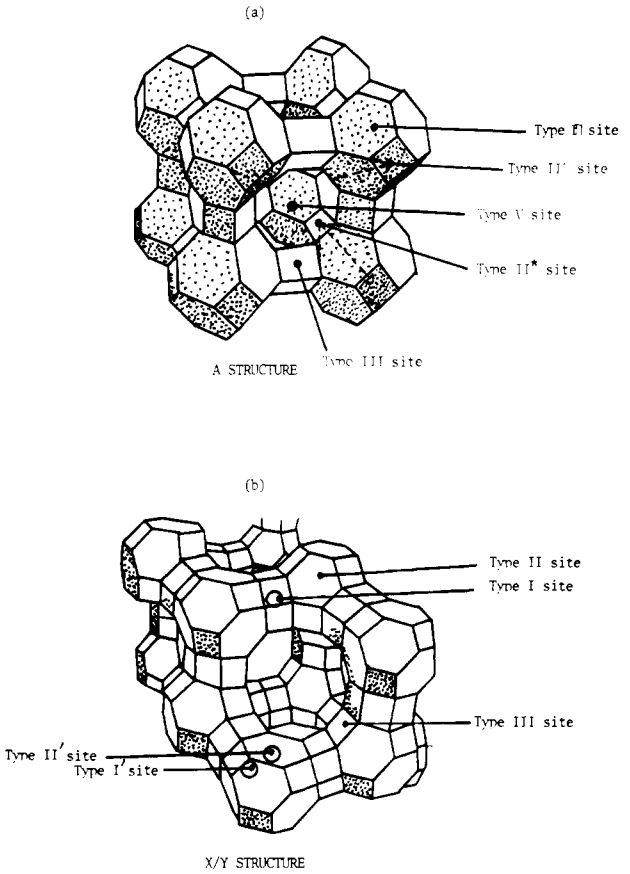

Figure 1. (a) Zeolite A structure. (b) Zeolite X/Y (Faujasite type) structure.

phase[25] with ferromagnetic properties.[20] The occurrence of fine-structure ESR signals together with the variety of coordination symmetries the Fe(III) ions experience in zeolitic structure and with the occasional possibility that the Fe(III) ions are involved in amorphous phases generated from structure breakdown of zeolite would produce a convolution of signals, especially when the line width of individual signals is relatively large. This convolution becomes broader in spectra of powders. Several workers attempted to analyze the convolution spectrum due to Fe(III) ions in zeolites into individual components. An important study toward this end is the work of Derouane and co-workers,[25] who followed changes in the ESR spectrum of Fe(III) impurities present in commercial zeolites with treatments that remove Fe(III) ions from the samples. From the spectra obtained after each leaching treatment, these workers were able to specify the g values of the various Fe(III) species present in these samples as follows: (1) Fe(III) ions replacing Al(III), at $g \simeq 4.3$ with a line width of 125 G; (2) Fe(III) ions in cationic sites, at $g \simeq 2.0$ with a line width of 250 G; (3) Fe(III) ions in Fe_3O_4 or occluded ferric salts (or precipitated compounds) with strong exchange spin–spin interaction at $g = 2.3$ with line widths of 1280 G. Some workers used the above findings in their search for breakdown, by following the signal assigned to ferromagnetic phases after certain processes[16,26] or treatments[20,27-29] of zeolitic structure. Furthermore, both Mössbauer and ESR spectra have been used to follow the redox behavior of Fe(III) ions in zeolites during dehydration.[17,20]

With the complicated ESR spectra of Fe(III) ions in the zeolitic structure it is rather difficult to draw conclusions by using this technique on its own for identification of the site of localization of Fe(III) ions. However, in ESR spectroscopy of Fe(III) ions there is the element of sensitivity, which makes the technique valuable in following changes of coordination symmetry of Fe(III) ions with treatments of zeolitic structure. Whenever the extent of a particular treatment produces a proportional change in some variable of the Fe(III) ions system, i.e. Fe(III) ion content increase, zeolitic structure breakdown, Si/Al ratio change, H_2O content decrease, $[Fe^{2+}]/[Fe^{3+}]$ increase, etc., it is possible to obtain interesting information about the change of variable just from changes in the ESR spectra of Fe(III) ions if its coordination symmetry is affected. With proper control of the treatment the percentage of variable change can be predicted or measured and the corresponding change in the ESR spectrum can be followed from measurements of intensity, g shift, line width, etc. in the spectrum, whichever is the most appropriate.

In this work two such variable changes are considered; one is the zeolitic structure, and the other one is the Fe(III) ion content. The former variable is extended between the crystalline structures of A and X type zeolites. These structure types were chosen because the X type structure has all the sites of A type and additionally sites of different coordination inside the truncated octahedra and hexagonal prisms. Therefore differences between spectra of Fe(III) ions in the two structures would reveal at least partial occupancy of sites of different coordination symmetry by Fe(III) ions in the two structures. Finally for both structures (A and X), a series of Fe(III) ion exchanged samples, with increasing Fe(III) ion content were investigated to follow the dependence of signal intensities, line widths, and shapes with the percentage of Fe(III) ion exchange.

Experimental Section

Materials. Na–Ca–A and Na–X molecular sieves were obtained from Union Carbide. $FeCl_3$, KSCN, and all other reagents used in chemical analyses were AnalaR grade. He and N_2 gases used in surface area measurements and ethylene gas used in adsorption measurements were of extra purity (BDH). The water used in this work unless otherwise specified was distilled.

Methods. Preparation. The preparation of Fe(III) ion exchanged zeolites was made by the following procedure, which was the outcome of previous investigations on the breakdown of zeolitic structure under conditions of Fe(III) ion exchange.[15] An aqueous solution of $Fe(SCN)_n^{(3-n)+}$ complex was prepared by bubbling HSCN (KSCN + HCl) through an aqueous solution of $FeCl_3$. The aqueous $Fe(SCN)_n^{(3-n)+}$ was extracted with ether and the ethereal HSCN + $Fe(SCN)_n^{(3-n)+}$ solution was used for the Fe(III) ion exchange of Na–Ca–A and Na–X as follows. The original zeolites were washed thoroughly with distilled water and were placed in a three-neck round-bottom flask equipped with a mechanical stirrer, a separating funnel containing the ethereal $Fe(SCN)_n^{(3-n)+}$ solution, and a thermometer. Distilled water was then added to produce a slurry, and the whole was stirred vigorously to ensure complete distribution of the two phases. The ethereal $Fe(SCN)_n^{(3-n)+}$ solution was added dropwise to avoid an excess of $Fe(SCN)_n^{(3-n)+}$ in aqueous phase. The aqueous phase of the slurry was not buffered to avoid an infinite proton source,[30] and therefore the pH decreased with increase of percentage of exchange between the values of 8 and 4 for Na–X and 7 and 5 for Na–Ca–A. The method resulted in an instantaneous exchange of Fe(III) ion content of each drop with the zeolite, thus leaving the liquid phase of the slurry colorless.[15] The Fe(III) ion exchanged zeolites were then filtered and washed several times until thiocyanate was not detected in the filtrate. The washed ion-exchanged zeolites were then evacuated in a vacuum oven at 80 °C. The partly dried zeolites were then stored in bottles and left to rehydrate. The water of the rehydrated samples was found to be between 20 and 21% by weight for Fe–5A samples and 24 and 25% by weight for Fe–13X samples.

Chemical Analyses. The hydrated Fe(III) ion exchanged zeolites were dried at 600 °C in a furnace and then were treated with H_2SO_4 (96%) and HF (48%) in Pt crucibles placed on steam baths to dissolve the zeolites. The obtained solutions were diluted with distilled water to 500 mL. The metal content (Na(I), Ca(II), Fe(III)) of the solutions was determined by atomic absorption spectrophotometry using standard methods.[31] Additionally the Fe(III) content of solutions was determined colorimetrically by using the standard method, which employs 4,7-diphenyl-1,10-phenanthroline reagent. Results of the chemical analyses

(25) Derouane, E. G.; Mestdagh, M.; Vielvoye, L. *J. Catal.* **1974**, *33*, 169.
(26) Mörke, W.; Vogt, F.; Bremer, H. *Z. Chem.* **1976**, *17*(5), 196.
(27) Wichterlová, B.; Kubelcová, L.; Novoková, J.; Jiřu, P. In *Metal Microstructures in Zeolites*; Jacobs, P. A., et al., Eds.; Elsevier: Amsterdam, 1982; p 142.
(28) Wichterlová, B. *Zeolites* **1981**, *1*, 181.
(29) Wichterlová, B.; Jiřu, P. *React. Kinet. Catal. Lett.* **1980**, *13*, 197.
(30) Schoonheydt, R. A.; Vandamme, L. J.; Jacobs, P. A.; Uytterhoeven, J. B. *J. Catal.* **1976**, *43*, 292.
(31) Evmerides, N. P.; Dwyer, J. *Chem. Chron.* **1982**, *1*, 331.

Table I. Metal Ion Content, Microporosity, Crystallinity, Adsorption, and Rate Measurements on Fe(III) Ion Exchanged Samples

sample	% exchange Na^+	% exchange Fe^{3+}	% exchange Ca^{2+}	% total exchange	residual SCN^-	microporosity: SSA, m^2	crystallinity: % retained	ethylene adsorption: ΔH, kcal/mol	rate const: CO oxidn,[b] mol of CO_2/(g s mol of CO)
Na–Ca–A	25.82 (24.8)[a]		75.00 (36.0)	100.8		688	100.0	12.1	0.2
Fe–5A(1)	19.35 (18.6)	4.17 (0.2)	75.50 (36.3)	98.0	[c]		103.0	11.3	
Fe–5A(3)	17.93 (17.2)	7.65 (0.3)	76.0 (36.6)	101.6	[c]		103.0	14.6	
Fe–5A(3)	16.25 (15.6)	10.50 (0.42)	70.5 (33.8)	97.2	[c]	675.5	100.0	10.89	
Fe–5A(4)	13.42 (12.9)	20.0 (0.8)	68.20 (32.5)	101.6	[c]	680	82.3	13.05	0.7
Na–X	94.00 (81.0)			94.0	[c]	869	100.0	8.96	0.5
Fe–13X(1)	94.00 (81.0)	7.33 (2.1)		101.3	[c]		103.0	9.29	
Fe–13X(2)	82.60 (69.3)	15.60 (4.5)		98.2	[c]		100.0	9.73	0.4
Fe–13X(3)	77.70 (66.8)	23.00 (6.6)		100.7	[c]	845	99.0	8.86	0.4
Fe–13X(4)	67.65 (55.0)	31.00 (8.9)		98.7	[c]	804	87.5	8.84	0.4
Fe–13X(J)	21.30 (18.3)	81.50 (23.4)		102.8	[c]	252	15.0		

[a] Numbers in parentheses give the number of Fe(III) ions per unit cell. [b] At 480 °C. [c] Not detectable.

are given in Table I as percentage of exchange. Detection of residual thiocyanate in zeolites was performed by (a) fusion of zeolite with Na_2CO_3 and SCN^- detection by anion standard methods, (b) combustion of the zeolite in air at 1200 °C and measurement of the evolved SO_2 titrimetrically,[32] and (c) measuring the intensity of the IR absorption band at 2060 cm^{-1}. In all cases the SCN^- residual content was found to be below the detection limit of the methods used.

Specific Surface Area Measurements. N_2 adsorption–desorption isotherms were obtained at 77 K with the volumetric method using conventional (Pyrex) glass cells and vacuum systems. Pressures were measured with mercury manometers and a cathetometer. The apparatus used was similar in design to that described by Lippens and co-workers[33] and the procedure followed in this work consisted of (a) evacuation of the sample at elevated temperatures, (b) estimation of dead space by introduction of He at 77 K to the evacuated sample and measurement of the pressure above it, (c) introduction of known amounts of N_2 at 77 °K and measurement of the partial pressures above it. The detailed procedure is described by Badran and co-workers.[24] The specific surface areas obtained are given in Table I.

Crystallinity Measurements. The X-ray spectra of powder samples of Fe(III) ion exchanged zeolites were obtained to get information about their internal structure. A Phillips diffractometer equipped with cobalt Kα radiation source was used. From separate investigations[24] it was found that the intensity of plane (111) for Na–Ca–A samples and (533) for Na–X were correlated to the percentage loss of crystallinity of the samples. The obtained percentage of crystallinity is tabulated in Table I for each sample.

Heats of Ethylene Adsorption. The adsorption properties of the zeolitic surface were measured from isosteric heats of adsorption of ethylene by using a katharometer (Pye Unicam) equipped with an integrator and a gas-sampling device. The Fe(III) ion exchanged zeolites were placed in glass chromatography columns, thus forming the static phase of the system while the ethylene was the mobile phase. From retention volumes of different size ethylene samples on the Fe(III) ion exchanged zeolites, the adsorption isotherms were obtained at various temperatures, and from the isotherms, the isosteric heats of adsorption were calculated and are given in Table I for each sample.

Rate Constants of CO Oxidation. The activity of zeolitic surface to the oxidation reaction of CO to CO_2 was measured by using a flow reactor of differential type. The catalyst was previously activated at 500 °C and the rate constants were obtained at 480 °C by using an O_2/CO concentration ratio of 1. No film diffusion was observed in specially designed tests. The obtained rate constants are tabulated in Table I for several samples.

ESR Measurements. The spectra were recorded on a Decca Type X1, X-band spectrometer, and the first derivative of absorption was recorded. The cavity, tuned to a klystron operation at 9270 MHz, contained a ruby crystal, which imposed standard signals at 1918 G (R_1), 2219 G (R_2), and 4873 G (R_3) on all spectra obtained and enabled g values to be determined. The field scan range of the spectra was from 100 to 6000 G, approximately. Special care was taken for the powder to be homogeneous in the sample holder and the bulk density of the powder to be the same for all samples so that the spectra are comparable. This was possible because the size of the particles in the powder were of the same dimensions in all samples since the original samples were of the same particle size.

Table II. Signal Intensities of Samples

sample	I(rel), arbitrary units $g \simeq 4.3$	I(calcd), arbitrary units $g \simeq 2.0$
Fe–5A(1)	2.7	7260
Fe–5A(2)	5.5	14200
Fe–5A(3)	4.1	16300
Fe–5A(6)	3.3	23520
Fe–5A(4)	2.4	31350
Na–X (bkgd)	4.6	2940
Fe–13X(1)	6.1	12900
Fe–13X(2)	8.1	18850
Fe–13X(3)	24.0	32400
Fe–13X(4)	40.0	41400
Fe–13X(J)	240.0	76400

Results

The ESR spectra obtained from Fe–5A and Fe–13X samples were similar in appearance and in the number of signals. Figure 2a,b shows the spectra obtained from samples of 5A and 13X, respectively. In spectra of Figure 2, the absorption lines marked with (R) are lines arising from the ruby crystal, which was used to give the reference absorption lines for relative intensity measurements and the g value marks for calibrating the magnetic field axis. The position of 2.0 and 4.3 values of g on the magnetic field axis are also marked on the spectra with arrows. From this figure it is shown that the spectra consist of a very broad signal centered at $g \simeq 2.0$ with a sharp signal about $g = 4.3$ superimposed on it. The shape of the broad signal does not change with the percentage of exchange. Intensity measurements of the sharp signal were calculated relative to the intensity of reference signals from the equation $I_r = h_s(\Delta H_s)/h_r(\Delta H_r)$, where h_s and h_r are the peak to peak height for the first derivative sample and reference signals, respectively, and ΔH_s and ΔH_r are the line widths of sample and reference signals respectively. Intensity measurements of the broad signal were calculated by using a numerical-integration method.[34,35] The intensity data of samples investigated in this work are shown in Table II in arbitrary units. The different headings between column 2 and 3 for relative intensities are given for the purpose of emphasizing the fact that the relative intensity at $g \simeq 4.3$ was obtained in a different way from that at $g \simeq 2.0$. The intensity data of Table II are plotted in Figure 3 against the percentage of exchange. At a relatively low percentage of exchange the intensities of the $g \simeq 2.0$ signal were found to follow a linear relationship of the form $Y_1 = a_1X$, where Y_1 = relative intensity, X = percentage of exchange, and a_1 = proportionality constant for both A and X type zeolites. The linearity might be assumed to hold to the higher percentages of Fe(III) ion exchange of Na–X type zeolites if the contribution (from introduced Fe(III) ion) to $g \simeq 4.3$ signal was negligibly small for all samples. On the other

(32) Cyganski, A.; Majewski, T. *Analyst (London)* **1979**, *104*, 167.
(33) Lippens, B. C.; Linsen, B. G.; de Boer, J. H. *J. Catal.* **1964**, *3*, 32.
(34) Wyard, S. G. *Gen. Sci. Instrum.* **1965**, *42*, 769.
(35) Ayscough, P. B. In *Electron Spin Resonance in Chemistry*, Methuen: London, 1967, p 451.

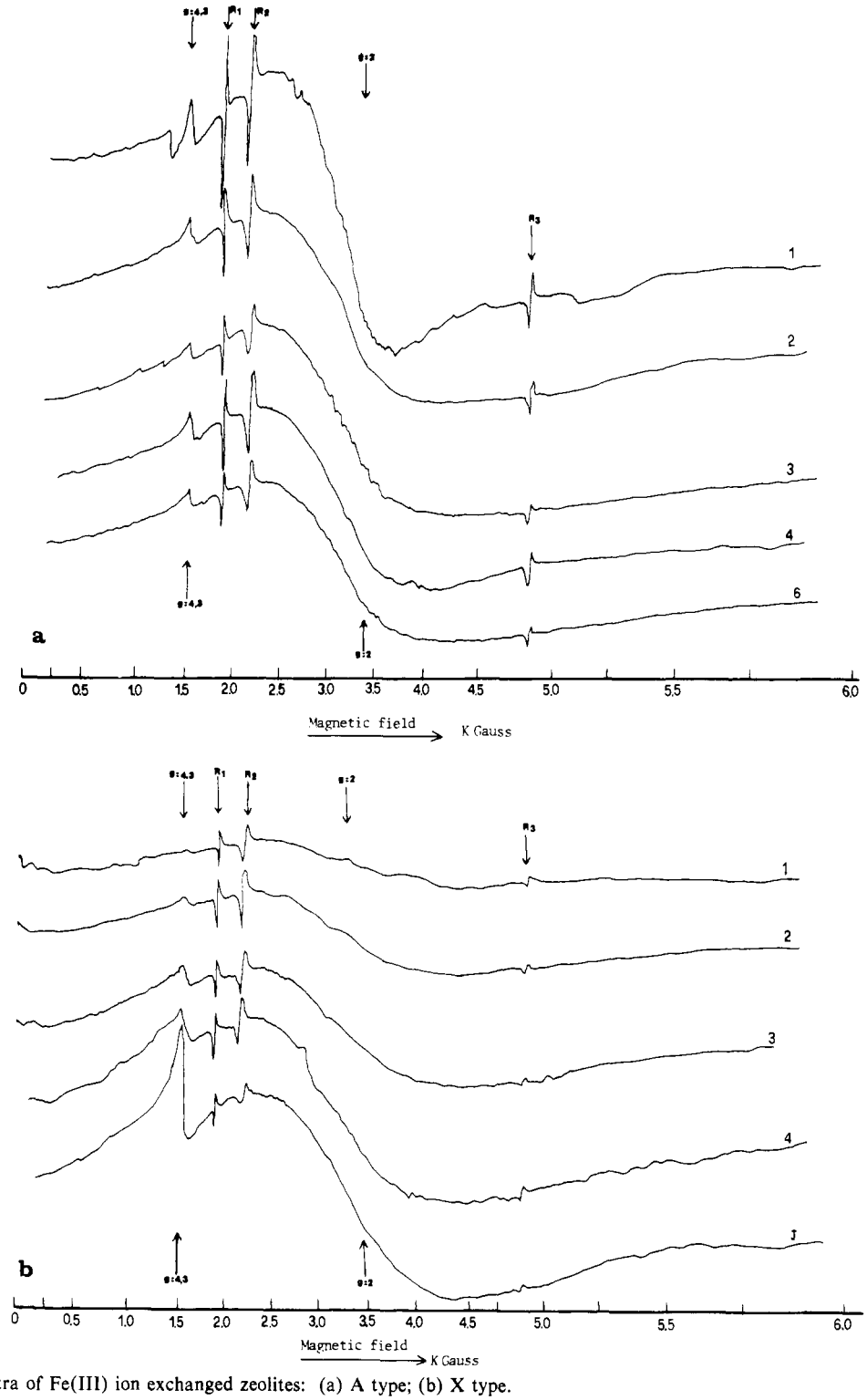

Figure 2. ESR spectra of Fe(III) ion exchanged zeolites: (a) A type; (b) X type.

hand results for the relative intensity of the $g \simeq 4.3$ signal of 13X samples, when plotted against percentage of exchange (Figure 3b), show a relationship $Y_2 = a_2X^2$, where Y_2 = relative intensity of the $g \simeq 4.3$ signal, X = percentage of exchange, and a_2 = proportionality constant. The points were also fitted to the linear relationship $Y_2/X = a_2X$ with a correlation coefficient of 0.993. On the contrary, in samples of A type zeolitic structure the intensity of this signal was not found to follow the increase of Fe(III) percentage of exchange but rather to remain constant and equal to that of the background in 5A level. Finally Table III tabulates data of signal intensity at $g \simeq 4.3$ together with the percent loss of microporosity and the percent loss of crystallinity found for the same samples.[15] The loss of microporosity was measured by sorption measurements while the loss of crystalline structure was obtained from X-ray intensity measurements. The last column of Table III tabulates percentage breakdown of zeolitic structure calculated from the relative intensity of $g \simeq 4.3$ signal, using the scale 4.6–239 relative intensity units for 0–80% breakdown, respectively.

Discussion

Signals of Fe(III) ion complexes in various matrices can be explained from the spin Hamiltonian of the $^6S_{5/2}$ state[36-41]

$$\mathcal{H} = g\beta HS + D[S_z^2 - \tfrac{1}{3}S(S+1)] + E[S_x^2 - S_y^2] \quad (1)$$

(36) Abragam, A.; Pryce, M. H. L. *Proc. R. Soc. London, A* **1951**, *205*, 135.
(37) Ingram, D. J. E. In *Spectroscopy at Radio Microwave Frequencies*; Butterworths: London 1967.

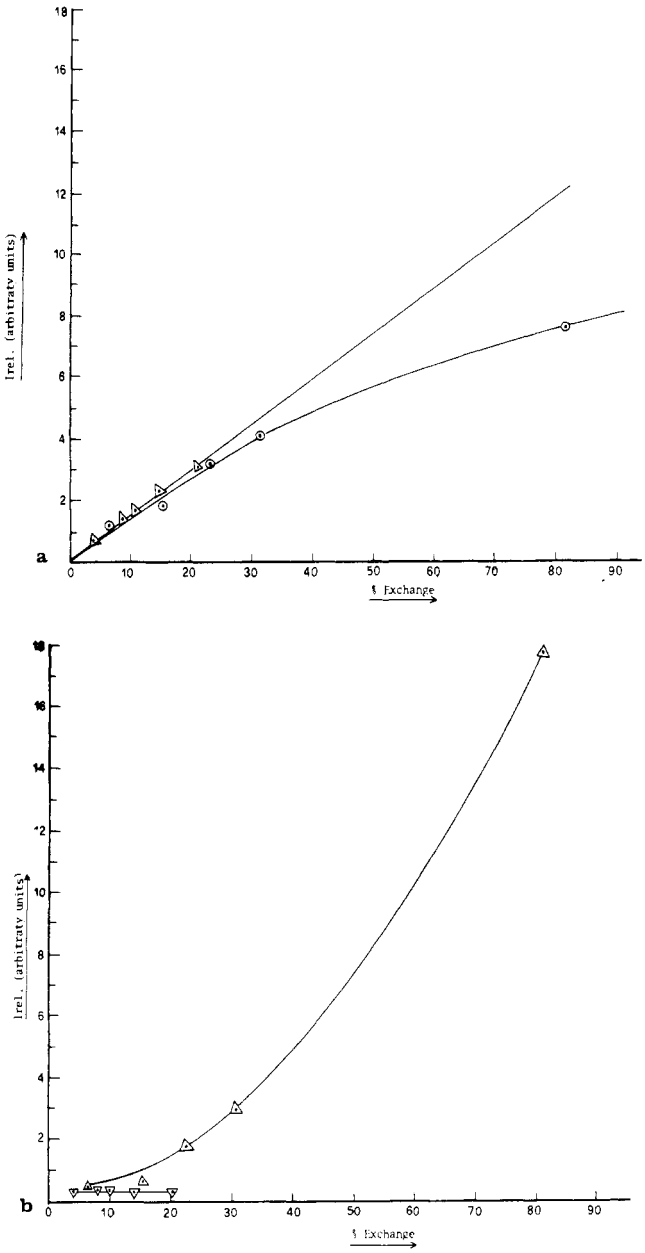

Figure 3. Correlation between the relative intensities and percentage of exchange for Fe–5A and Fe–13X samples: (a) signal at $g = 2.0$; (b) signal at $g = 4.3$.

Table III. Signal Intensity at $g \simeq 4.3$ and Calculated Sample Breakdown in Comparison with Loss of Microporosity and Loss of Crystallinity

sample	% loss of microporosity[a]	% loss of crystallinity[b]	I(rel) at $g = 4.3$	% breakdown
Na–X			4.58	
Fe–13X(1)			6.13	0.5
Fe–13X(2)			8.06	1.2
Fe–13X(3)	2.0	1.0	23.9	6.6
Fe–13X(4)	8.0	12.0	40.0	12.1
Fe–13X(J)	71	85.0	239	80.0

[a] From nitrogen sorption. [b] From X-ray diffraction.

where $g = 2.0$, β = Bohr magneton, H = magnetic field intensity, S = electronic spin, S_x, S_y, and S_z are the components of the electronic spin vector along the x, y, and z directions of the crystal field, and D and E are the axial and rhombic distortion parameters of the zero-field-splitting (zfs) interaction.[42] The first term in eq 1 is the Zeeman interaction and is written for the isotropic **g** tensor, which is invariant with changes in orientation of the sample in the magnetic field. The second and third terms of eq 1 are anisotropic and their effect will be orientation-dependent. In rapidly rotating complexes (i.e. $\Delta\omega(\tau_r) < 1$, where $\Delta\omega$ is the zfs in angular frequency units and τ_r is the rotational correlation time) the zfs is averaged to zero. Consequently, transition frequencies of the fine structure components are equal and the spectrum is a simple isotropic signal. When rotational motion is slow or the zfs large, $\Delta\omega(\tau_r) > 1$, the terms in D and E no longer average to zero, and ESR spectra of more than one transition are obtained. In such cases the zfs interaction produces characteristic shifts in the energy levels of the spin system,[42,43] which are manifested in the spectrum as fine-structure transitions displaced from the unperturbed or isotropic resonance position (H_0).

The limiting cases[38] of eq 1 are as follows: (i) $D = 0$ and $E = 0$, an isotropic signal of $g = 2.0$ or slightly greater value is observed;[44] (ii) $D \neq 0$ and large and $E = 0$, an anisotropic signal is observed[45] with $g_\parallel = 2.0$ and $g_\perp = 0$; (iii) $D = 0$ and $E \neq 0$, an isotropic signal is observed with $g = 4.29$. The coordinations corresponding to this last signal ($g = 4.29$) include tetrahedral MA_2B_2 (C_{2v}), distorted octahedral MA_6 (D_{2h}) or MA_3B_3,[46,47] where M = metal ion and A and B = ligands.

The samples used in this work were checked for structure breakdown with X-ray diffraction and sorption measurements. All samples were found to retain their zeolitic crystal structure except the sample Fe–13X(J), which was almost completely broken down. X-ray powder patterns of samples before and after sample pretreatment were identical, showing no sign of loss of crystallinity during this mild treatment and no extra lines were observed in the X-ray spectra of the samples, apart from those due to zeolitic structure. The samples were also checked for occlusion of Fe(III) salts during the ion-exchange process by correlating the loss of Na(I) with the gain of Fe(III). In all cases it was found that ionic balance was achieved, indicating stoichiometric exchange. Because the pH during the ion-exchange process was sufficiently high to exclude the possibility of zeolite structure collapse due to protonic attack and because the ion exchange process was carried out under mild conditions of temperature and metal ion concentration, it is assumed that the ion-exchange process was not accompanied by a parallel process of zeolite structure modification. Any contributions from soluble hydrolysis products of Fe(III) ions which could be ion exchanged should be negligible because of the stoichiometry observed. Furthermore the heats of adsorption of ethylene and the surface activities of Fe(III) ion exchanged zeolites to CO oxidation reaction as shown in Table I are not, in general, significantly different from the values for unexchanged zeolites (Na–Ca–A, Na–X) thus ensuring the absence of the Fe_2O_3 phase on the external surface of the zeolite,[48] which is formed by heat treatment of $Fe(OH)_3$ deposited on the zeolite surface. Therefore, ESR spectra of these samples may be regarded as representing the ion-exchanged Fe(III) ions in the zeolitic phase or Fe(III) ions involved in other phases (amorphous) generated from an initially ion-exchanged zeolitic phase (particularly in case of sample J, which was largely amorphous).

Sample pretreatment (dehydration at less than 100 °C under water pump vacuum and gradual rehydration during long storage in bottles) ensures that Fe(III) ions in zeolitic phase are partly coordinated to zeolitic oxygens in sites near the walls of the supercage.[23] Such sites exist in both zeolitic structures, some of which are close to O_1 structural oxygens.[49] Optical spectra have

(38) Dowsing, R. D.; Gibson, G. F. *J. Chem. Phys.*, **1969**, *50*, 294.
(39) Aasa, R. *J. Chem. Phys.* **1979**, *52*, 3919.
(40) Griscom, D. L.; Griscom, R. E. *J. Chem. Phys.* **1967**, *47*, 2711.
(41) Reed, G. H.; Ray, W. J., Jr. *Biochemistry* **1971**, *10*, 3194.
(42) Bleaney, B.; Trenam, R. S. *Proc. R. Soc. London, A* **1954**, *1*, 223.
(43) Hurd, F. K.; Sachs, M.; Hershberger, W. D. *Phys. Rev.* **1954**, *93*, 373.
(44) Orton, J. W. *Rep. Prog. Phys.* **1959**, *22*, 204.
(45) Bennett, J. E.; Gibson, J. F.; Ingram, D. J. E.; Hanghton, T. M.; Kerkut, G. A.; Munday, K. A. *Proc. R. Soc. London, A* **1961**, *262*, 395.
(46) Loveridge, D.; Parks, S. *Phys. Chem. Glasses* **1971**, *12*, 19.
(47) Griffith, J. S. *Mol. Phys.* **1964**, *8*, 213, 218.
(48) Mortier, W. J.; Schoonheydt, R. A. *Prog. Solid State Chem.* **1985**, *16*, 2.
(49) Beagley, B.; Dwyer, J.; Evmerides, N.; Hawa, A. I. F.; Ibrahim, T. K. *Zeolites* **1982**, *2*, 167.

shown square-pyramidal or distorted-octahedral[23] (elongated along fourfold axis) coordinations. Such coordinations are characterized by low symmetry, which imposes a zfs interaction and gives spectra with fine structure. Fine structure transition g values for Fe(III) ions show angular dependence.

When the crystal field effects are sufficiently weak or the operating frequency is sufficiently great, the fine structure interaction can be treated by perturbation theory. In ground states with half-integral multiple electronic spin, there is a central ($M_s = -1/2 \leftrightarrow M_s = +1/2$) transition that is affected only by second-order fine-structure terms, flanked by satellite lines belonging to the rest of the transitions that are affected by both first- and second-order terms. This splitting of transitions becomes greater with increasing S value.

Powder spectra are spectra of randomly oriented spins in the steady magnetic field. Each transition in the powder spectra will be spread over a wide range of H values due to a dependence of the transition line position on the angles θ and ϕ to form the so called powder pattern. The spread is greater for satellite lines, which are in fact lost in the noise level when the spin system has high S value. In such spin systems the only observable powder pattern is composed of the central transition. The apparent spread of the spectrum will be due to the powder pattern of the central transition line, which is given by eq 2.

$$\Delta H_{FS} = (D^2/36g^2\beta^2H_0)[S(S+1) - 3/4] \times [9(E/D)^2 + 66(E/D) + 25] \quad (2)$$

Consequently the width of the overall signal depends mainly on the size of the D value and to a lesser extent on E/D. Such a spectrum is formed from an envelope of signals with shoulders at $-9(1 + E/D)^2$ and $16[1 + (3E/D)]$ and divergencies at $16[1 - (3E/D)]$ and $-9[1 - (E/D)]^2$ or $-8[1 - (E/D)]^2$ (depending on whether the E/D value is less than or greater than $1/9$) on the axis of $H - H_0$ and in units of $(D^2/36g^2\beta^2H_0)$ $[S(S+1) - 3/4]$. The dipolar interaction increases the individual line width and makes the overall spread larger. Powder patterns may show larger spread when D and E/D parameters belong to distributions of such values around a central value. Such a case was reported by Burlamachi,[50] who suggested that loose water molecules provide collisions through Brownian motion to metal ions coordinated to ligands and therefore disturb their coordination symmetry. If we denote the correlation time of such collisions by τ_c and the correlation time of reorientation by τ_r and if $\tau_c > \tau_r$, then at a given moment different paramagnetic ions experience different crystal field anisotropies.

The experimental spectra shown in Figure 2a,b are very broad signals with g values around 2.0. Superimposed on this broad signal is a sharper signal positioned at $g \simeq 4.3$. Because of significant broadening of the individual lines, the powder spectra do not show clearly resolved all singularities of the powder pattern. Observations made on shapes, spread of powder pattern, and relative intensities of the broad signal of samples having different percentages of Fe(III) ion exchange showed the following.

(1) Among samples of the same crystalline structure the shape is not changed, but the line width is increased slightly due to increase of dipolar interactions. Pairing or clustering could be another source of broadening, but the Mössbauer technique does not indicate such a process,[22] at least at percentages of exchange as high as 50%.

(2) Among samples having the A and X crystalline structure, the shapes and line widths are almost the same.

(3) At a relatively low percentage of exchange, where there is no contribution from Fe(III)-exchanged ions to the $g \simeq 4.3$ signal for Fe–5A samples or a negligible contribution for Fe–13X samples, the relative intensity of the broad signal is linearly related to the percentage of exchange (Figure 3a) for the samples of both A and X type zeolitic structures.

(4) The linearity coefficient, a_1, is approximately the same for both structures (Figure 3a).

(50) Burlamachi, L. *J. Chem. Phys.* **1973**, *58*, 3609.

Relative intensities are proportional to the energy of absorption from the oscillating resonance field dw/dt, which is related to the transition frequency, W_{ij}, by the equation[51]

$$dw/dt = W_{ij}(h\omega)(N_i - N_j) \quad (3a)$$

where N_i and N_j = populations of ground and excited states, respectively, and ω = frequency expressed as angular velocity. The transition frequency, however, is related to transition probability with the equation

$$W_{ij} = \frac{\pi H_1^2}{2\hbar^2}|M_{ij}|^2 f(\omega) \quad (3b)$$

where H_1 = amplitude of the oscillatory field, $|M_{ij}|^2$ = the transition probability, and $f(\omega)$ = the shape function. From all the factors in eq 3a,b, the factor that changes within the ESR experiment is the transition probability, which for a given transition depends upon the symmetry.

The transition probability is mainly dependent on the M_s value of the transition, and in cases where anisotropic tensors are involved in the spin Hamiltonian, it depends on expressions of orientations of the principal axes of these tensors to the direction of the steady magnetic field and oscillatory resonance field. A simple expression between the relative intensity of a given transition and the concentration of Fe(III) ions in the zeolite, [Fe(III)–Zeol], could be given from

$$Y_1 = k_1[\text{Fe(III)–Zeol}] \quad (4)$$

where k_1 = constant depending on anisotropy of **g**, **D**, etc. tensors, and $N_i - N_j$ is to be proportional to the Fe(III) concentration in the zeolite. A linear relationship between the relative intensity of a given transition and the total percentage of exchange provides evidence for a single type of Fe(III) coordination symmetry or less likely an identical distribution among the sites for the whole range of percentage of exchange (Appendix).

The acceptance of the linearity of relative intensity of the $g \simeq 2.0$ signal as an evidence for a single type coordination symmetry for Fe(III) ions contributing to this signal, together with the previous discussion of powder patterns for $^6S_{5/2}$ ground state in low coordination symmetry, leads to the assignment of this signal to the powder pattern of the central transition $M_s = +1/2 \leftrightarrow M_s = -1/2$ of a low coordination symmetry Fe(III) ion. Taking into account the width of this signal (spread of powder pattern), which is around 1600 G, the $D/h\nu$ value is calculated to be within the range 0.21–0.29 if E/D is allowed to take some value between 0 and $1/3$. However, the derivative spectrum of this transition is so broadened by dipolar interactions or other broadening mechanisms that singularities of the powder pattern are not resolved in the spectra. The assignment, therefore, of the E/D value is uncertain, and only a weak indication that $E/D > 1/9$ is provided from the more prolonged absorption in the high-field wing of the signal than in the low-field wing. In fact it is even likely that the spectra represent a distribution in crystal field parameters both in $D/h\nu$ and E/D.[52] The concept of a single coordination symmetry of Fe(III) ion in exchanged zeolites combined with the concept of the distribution of crystal field parameters leads to the conclusion that the localization sites are in the supercage of zeolitic structure where the Brownian motion of loose water molecules perturbs the coordination symmetry of the Fe(III) ion.

Although the broad signal is the main signal of the spectrum, a few sharp signals are observed on top of the broad signal, most of which are present only in one or two spectra (i.e. a signal at $g = 5.0$ in spectrum 1 of Figure 2a) and can be considered either as signals belonging to impurities (Mn^{2+}) of Na–Ca–A or Na–X or odd signals. However, the sharp asymmetric signal at $g \simeq 4.3$ is a prominent feature of all spectra obtained in this work and therefore is a signal contributed from Fe(III) ions. A value of

(51) Abragam, A.; Bleaney, B. *Electron Paramagnetic Resonance of Transition Metal Ions*; Oxford University Press: London, 1970; Chapter 3.
(52) Evmiridis, N. *Anal. Chim. Acta*, in press.

$g \simeq 4.3$ is obtained from eq 1 for the central transition $M_s = +^1/_2 \leftrightarrow M_s = -^1/_2$ when $D = 0$ and $E \neq 0$[38] or when $D/h\nu > 0.35$ and $E/D = {}^1/_3$.[39] Such signal at $g \simeq 4.3$ has also been observed in amorphous materials (e.g. glasses).[53] If this signal is compared in spectra of A and X type zeolites, it is clear that this signal increases with the percentage of exchange in X type zeolites, while in A type zeolites it remains constant at the background level (Na–Ca–A sample). The $g \simeq 4.3$ signal, in A type Fe(III) ion exchanged zeolites and in the unexchanged Na–X sample, is due to Fe(III) impurities in the reagents used for the synthesis of zeolites, and it has been assigned by various researchers[25,54] to Fe(III) ions that replace Al(III) ions from the zeolite framework and therefore are found in C_{2v} tetrahedral coordination symmetry. However, this signal in Fe(III) ion exchanged zeolites of the Na–X type cannot be assigned to Fe(III) ions replacing Al(III) from the zeolite framework because this is not energetically favorable and does not happen in Na–Ca–A Fe(III) ion exchanged zeolites. The intensity of this signal ($g \simeq 4.3$) is plotted against the percentage of ion exchange in Figure 3b. The smooth curve through the experimental points of X type zeolite is found to obey the relationship

$$Y_2 = a_2X^2 \tag{5}$$

where Y_2 = relative intensity of absorption signal at $g = 4.3$, X = total percentage of exchange, and a_2 = a constant factor depending on the conditions of ion exchange.

Equation 5 is interesting, and some physical meaning could be given by referring to either the ion-exchange process or possible solid reactions among [Fe(III)–Zeol] species formed from the ion exchange as follows.

(a) Ion-Exchange Process. A reasonable way to describe the ion-exchange process followed is by following chemical equilibria

$$\mathrm{Fe(SCN)}_n^{(3-n)+}(\mathrm{ether}) \rightleftharpoons \mathrm{Fe(SCN)}_n^{(3-n)+}(\mathrm{aq}) \rightleftharpoons \mathrm{Fe}^{3+} + n\mathrm{SCN}^-$$

$$\mathrm{SCN}^- + \mathrm{H_3O}^+ \rightleftharpoons \mathrm{HSCN} + \mathrm{H_2O} \tag{6}$$

$$\mathrm{Fe}^{3+} + n\mathrm{H_2O} \overset{\text{hydrolysis}}{\rightleftharpoons} \mathrm{P_i} + n\mathrm{H}^+$$

where P_i = $Fe(OH)^{2+}$, $Fe(OH)_2^+$, $Fe_2(OH)_2^{4+}$, or polymeric species, with hydrolysis equilibrium constant[55], K_i of 1×10^{-3}, 5×10^{-7} and 1×10^{-3}, respectively for the former water-soluble ferric ion species. Insoluble polymeric species do not contribute to the ion-exchange process while the soluble species ($Fe(OH)^{2+}$, $Fe(OH)_2^+$, $Fe(OH)_2^{4+}$, etc.) can enter the zeolite structure by ion exchange when their size is appropriately small, according to the ion-exchange chemical equilibrium equation

$$\mathrm{P_i}^{\nu+} + \mathrm{Na}_r\mathrm{Z} \rightleftharpoons \mathrm{P_iNa}_{r-\nu}\mathrm{Z} + \nu\mathrm{Na}^+ \tag{7}$$

From the equilibria mentioned above and the assumption that hydrolysis equilibria are very fast compared with ion exchange, we can derive equations that give the concentration of each P_i in the zeolite phase in terms of the analytical concentration of Fe(III) ions in aqueous solution, the hydrolysis constants, and distribution factors (here regarded independent of the concentration of hydrolysis products).

The relative intensity of the signal can then be related to the concentration of the hydrolysis product in the zeolite phase by equations having the form of eq 4. From the species considered, the $Fe_2(OH)_2^{4+}$ species provide relationship of type given in eq 4, which can take the form of eq 5 provided that the concentrations of all polymeric hydrolysis products and $Fe_2(OH)_2^{4+}$ species in the zeolitic phase are negligible compared to those of other species. Such an explanation would assign the $g \simeq 4.3$ signal to ion exchange of $Fe_2(OH)_2^{4+}$ species.

(b) Solid Reaction. In this case it is suggested that the species that contribute to the signal at $g \simeq 4.3$ have been generated from the reaction of Fe(III) ions in the zeolitic phase after they have been exchanged. A reaction in the solid zeolitic phase between Fe(III) ion exchanged species following the equation

$$2[\mathrm{Fe(III)–Zeol}] \underset{\mathrm{H_2O}}{\overset{K}{\rightleftharpoons}} (\mathrm{Fe_2O_3})_z \tag{8}$$

could produce a solid amorphous phase and might involve zeolite breakdown. The relative intensity of the signal contributed from the amorphous phase will satisfy

$$Y_2 = k_2[(\mathrm{Fe_2O_3})_z] = k_2K[\mathrm{Fe(III)–Zeol}]^2 = aX^2$$

which is identical with eq 5, where "a" is a constant that depends mainly on the equilibrium constant of reaction 8. This explanation for the form of eq 5 is based on the production of $(Fe_2O_3)_z$ from Fe(III) and is not limited by constraints such as those made in the case based on an ion-exchange process involving $Fe_2(OH)_2^{4+}$ species. Furthermore, various researchers[27–29] who examined the hydrothermal treatment of zeolites usually find an amorphous phase associated with Fe(III) ions, following this treatment.

Between these two cases, the data obtained in this work and other works seem to favor the explanation based on the solid-phase reaction for the form of eq 5 that was observed experimentally. For instance from the experimental work that has been reported by Wichterlová et al., the intensity of the signal at $g \simeq 4.3$ does not change with the pH of the aqueous medium in which the ion-exchange process takes place. Since the concentration of $Fe_2(OH)_2^{4+}$ species tends to increase with pH decrease, in the experimental range of pH 4–7, we could expect an increase in the intensity of the $g \simeq 4.3$ signal with such a decrease in pH, which is not observed. Also the ESR signal appears very much sharper than the one of $g \simeq 2.0$, which indicates that the spin–lattice relaxation time is much more different from the broad signal assigned to Fe(III) ions in the zeolitic phase. Finally, amorphous phases involving Fe(III) ions do appear during ion exchange, structure breakdown has been measured from the percentage loss of microporosity and the percentage loss of crystallinity[24] of these samples, and results are given in Table III. From values in Table III it is clear that the intensity of this signal tends to be correlated with the loss of microporosity and/or crystallinity. Assuming that percentage breakdown is proportional to the relative intensity of the signal at $g \simeq 4.3$ for the Fe(III) samples and setting the 0 and 80% breakdown at values of 4.6 and 239 units of relative intensity, respectively, we are able to find the percentage breakdown of all the 13X samples studied from the ESR spectra. The results are tabulated in the final column of Table III. The agreement between calculated percentage breakdown and percentage loss of microporosity or crystallinity is reasonable. Also for Fe(III) ion exchanged samples of A type zeolites where this signal did not increase with ion exchange it was found by the sorption and X-ray diffraction measurements that structure breakdown did not take place. This major difference between zeolites A and X in structure breakdown with Fe(III) ion exchange concerns the availability of ion sites within the small pore region which is well established for zeolite X (I, I′, and II′) but not for zeolite A. Consequently in the case of zeolite X we can envisage ferric ions in both small- and large-pore ion sites. This can facilitate arrangements where ferric ions are in the proximity of a common framework oxygen atom. However, framework O_1 has been found to show a greater tendency to be removed by interaction forces of metal ions.[56] The extensive polarization at this oxygen by two triply charged cations would, presumably, be a source of weakness and consequently a point of likely structure breakdown.

Acknowledgment. I thank M. MacDonald for running the ESR spectra and Dr. J. C. Vickerman, Dr. T. Parker, and J. Dwyer for helpful suggestions.

(53) Castner, T., Jr.; Newell, G. S.; Holton, W. C.; Slichter, C. P. *Chem. Phys.* **1960**, *32*, 668.
(54) McNicol, B. D.; Pott, G. T. *J. Chem. Soc. D* **1970**, *146*, 438.
(55) Kolthoff, I. M., Sandell, E. B., Meehan, E. J., Brunchenstein, S. Eds.; *Quantitative Chemical Analysis*, 4th ed.; Macmillan: New York, 1969.
(56) Evmerides, N. P.; Dwyer, J.; Parish, R. V. *Inorg. Chim. Acta* **1983**, *75*, 229.

Appendix

Assuming that the overall signal intensity is the result of two coordination symmetries, the total signal intensity (I) will be the sum of the relative intensities of the individual signals (I_1, I_2).

$$I = I_1 + I_2 \quad (9)$$

With $I_1 = k_1$[Fe(III)–Zeol$_1$] and $I_2 = k_2$[Fe(III)–Zeol$_2$]

$$I = k_1[\text{Fe(III)–Zeol}_1] + k_2[\text{Fe(III)–Zeol}_2] \quad k_1 \neq k_2 \quad (10)$$

If [Fe(III)–Zeol$_F$] is the concentration of Fe(III) ion in the fully ion-exchanged zeolite, then

$$[\text{Fe(III)–Zeol}_i] = \lambda_i[\text{Fe(III)–Zeol}_F] \quad (11)$$

where λ_i is the percentage of exchange from Fe(III) ions in site i, and from eq 9–11

$$I = (\lambda_1 k_1 + \lambda_2 k_2)[\text{Fe(III)–Zeol}_F] \quad (12)$$

Since $\lambda_1 + \lambda_2 = X$ = total Fe(III) percentage of exchange, it is clear that linearity of I with X is only obtained when $k_1 = k_2$ or when all Fe(III) ions belong to the same coordination symmetry.

An alternative explanation, less likely, is that the relative site occupancy remains the same as Fe(III) concentration increases.

Registry No. CO, 630-08-0; ethylene, 74-85-1.

Contribution from the Department of Chemistry, University of Michigan, Ann Arbor, Michigan 48109

Synthesis and Crystal and Molecular Structure of Trimethylammonium 7,8-Dimercapto-7,8-dicarbaundecaborate(10) and Trimethylammonium *anti*-7,7′:8,8′-Bis(dithio)bis(7,8-dicarbaundecaborate(10))

C. Viñas,† W. M. Butler, F. Teixidor,*† and R. W. Rudolph‡

Received April 30, 1986

Removal of B3 in 1,2-dimercapto-*o*-carborane is achieved when its ammonium salt is refluxed in ethanol in the presence of NaI. Upon addition of NMe_3HCl in water, trimethylammonium 7,8-dimercapto-7,8-dicarbaundecaborate(10) is precipitated. The NH_4^+ ion seems to act both as the source of the proton and as the base that removes B3. This compound, 7,8-$(SH)_2$-7,8-$C_2B_9H_{10}^-$, has been characterized by microanalysis, ^{11}B NMR spectroscopy, and an X-ray crystal structure determination. Crystals of NMe_3H[7,8-$(SH)_2$-7,8-$C_2B_9H_{10}$] are monoclinic, space group $P2_1/a$, with a = 14.711 (2) Å, b = 9.609 (2) Å, c = 10.604 (1) Å, β = 90.64 (1)°, and Z = 4. The anion 7,8-dimercapto-7,8-dicarbaundecaborate(10) has the form of an 11-apex fragment of an icosahedron with an ortho disposition of the C atoms in the open face with two exocluster sulfurs, one bonded to C7 and the other one to C8. Open-face distances of 7,8-$(SH)_2$-7,8-$C_2B_9H_{10}^-$ are compared to those of 9,10,11-Me_3-7,8-$C_2B_9H_9^-$ and discussed. A good correlation has been found between these distances and the bond orders in the cyclopentadienide anion and butadiene. The reaction of [7,8-$(SH)_2$-7,8-$C_2B_9H_{10}$]$^-$ with I_3^- yields 7,7′:8,8′-bis(dithio)bis(7,8-dicarbaundecaborate(10)). The structure of this anion, as the trimethylammonium salt, has been characterized by single-crystal X-ray diffraction methods. Crystals of $(NMe_3H)_2$[(7,8-$(S)_2$-7,8-$C_2B_9H_{10})_2$] are monoclinic, space group $P2_1/a$, with a = 13.318 (4) Å, b = 15.432 (5) Å, c = 7.084 (2) Å, β = 100.45 (2)°, and Z = 2. The anion consists of two 7,8-dicarbaundecaborate(10) moieties bridged by two –S–S– units in such a way that there is an inversion center in the middle of the molecule. Reaction of [(7,8-$(S)_2$-7,8-$C_2B_9H_{10})_2$]$^{2-}$ with $CoCl_2$ and cyclopentadiene yields *trans*-[(η^5-C_5H_5)(3,1,2-$CoB_9C_2S_2H_9$)]$_2$.

Introduction

Many *o*-carborane derivatives are known as a consequence of the high resistance of the *o*-carborane cage to chemical attack.[1] However, Hawthorne and co-workers discovered that B3 can be selectively removed from the cage by using a strong base, such as CH_3O^- in methanol.[2] Other nucleophiles are known to act in the same fashion, among them piperidine and trialkylamines.[1] The nucleophilic attack takes place at B3 (or B6) because these atoms are adjacent to the more electronegative atoms C1 and C2. It is hypothesized that an increase in the electron-withdrawing ability of C1 and C2 will facilitate B3 (or B6) removal). This may be observed in 1,2-dihalo derivatives degraded by both methanol and ethanol.[3] Though the electron-withdrawing ability of the substituted carbons may well explain these cases, it does not explain the observed partial degradations[4] in 1,2-dimercapto-*o*-carborane salts. We have recently reported that partial degradation of the *o*-carborane moiety happens when either ammonium or potassium salts of *o*-carborane-1,2-dithiolate react with dihaloalkanes[5] (see eq 1).

It was proposed that some stabilization may be acquired through the delocalization of the sulfur lone pair into the open-face orbitals of the partially degraded cage. Because partial degradation had been observed only when rings were formed, it was inferred that ring formation was a necessary, but not sufficient, condition for the partial degradation to occur.

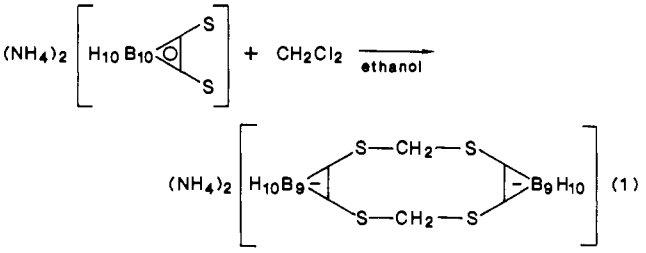

(1)

Herein we describe the synthesis and characterization of 7,8-dimercapto-7,8-dicarbaundecarborate(10) salts from the ammonium salt of 1,2-dimercapto-*o*-carborane. Contrary to what we initially thought, the partial degradation of *o*-carborane-1,2-dithiolate (ammonium salt) takes place without ring formation. In addition, the syntheses and characterization of *anti*-7,7′:8,8′-bis(dithio)bis(7,8-dicarbaundecaborate(10)) and *trans*-[(η^5-C_5H_5)(3,1,2-$CoB_9C_2S_2H_9$)]$_2$ are reported.[6]

Experimental Section

General Procedures. Before use, *o*-carborane (Dexsil Chemical Corp.) was sublimed; 1,2-dimercapto-*o*-carborane (I) was prepared from *o*-

†Permanent address: Divisió Inorgânica, Departament de Química, Universitat Autònoma de Barcelona, Bellaterra, Barcelona, Spain.
‡Deceased May 1981.

(1) Grimes, R. N. *Carboranes*; Academic: New York, 1970.
(2) Wiesboeck, R. A.; Hawthorne, M. F. *J. Am. Chem. Soc.* **1964**, *86*, 1642–1643.
(3) Zakharkin, L. I.; Podvisotskaya, L. S. *Izv. Akad. Nauk. SSSR, Ser. Khim.* **1966**, 771.
(4) By partial degradation we mean removal of B3, yielding 7,8-dicarbaundecaborate derivatives.
(5) Teixidor, F. T.; Rudolph, R. W. *J. Organomet. Chem.* **1983**, *241*, 301–312.
(6) A preliminary report has been published. See: Viñas, C.; Butler, W. M.; Teixidor, F.; Rudolph, R. W. *Organometallics* 1984, *3*, 503.

0020-1669/86/1325-4369$01.50/0